Section: Research Paper

STRUCTURE STABILTY , SPECTROSCOPIC, OPTOELECTRONIC PROPERTIES AND MOLECULAR DOCKING INVESTIGATIONS OF M-NITROPHENOL USING MOLECULAR MODELING

S.Sindhuja[a], M. Karnan[a] R.Gayathri[b] and R. Elayaraja[c]

[a]PG and Research Department of Physics, Srimad Andavan Arts & Science College (Autonomous) affiliated to bharathidasan university, Trichy, Tamil Nadu, India.

[b]PG and Research Department of Physics, Cauvery College for Women(Autonomous) affiliated to bharathidasan university, , Trichy, Tamil Nadu, India.

[c]Department of Physics, Sri Meenakshi Vidiyal Arts and Science College, Trichy, Tamil Nadu, India.

[a]ssindhujaphysics@gmail.com

Abstract

M-Nitrophenol was subjected to ab initio and DFT conformational analysis. The structural characteristics of the M-Nitrophenol and the stability and Molecular Properties have been Analysed using geometrical tools. It was revealed that sparsely spaced hydroxyl groups, especially those with hydrogen bond-like interactions, reduced the P.E. minimum for the molecules. It was also discovered that steric interference between closely positioned functional groups across the phenyl and nitro groups was one of the reasons capable of compromising co-planarity. Nevertheless, studies on new flavonoids revealed that the unpaired electron is restricted solely to the ring and is not delocalized across the phenyl ring. Moreover, chemical reactivity in the condensed Fukui function, as well as the molecule's MEP and HOMO-LUMO energies, were studied. The inter- and intramolecular charge transfer interactions responsible for biological activity were investigated using orbital analysis. Docking study reveals four non-polar hydrogens and six aromatic carbons, each with two rotatable bonds. The ligand and protein were saved in PDBQT format using Autodock. The ligand-receptor interaction had a magnitude of -10.03 kcal/mol. A hydrogen bond is formed by the active site (ARG50A) N-H bonds, (Lys55A) N-H bonds of 1SOH and two N-O of OPTIFREQ, and (ARG50A) N-H bonds of 1SOH and O of OPTIFREQ with bond lengths of 2.2, 2.2, and 2.5. In addition, the chemical reactivity

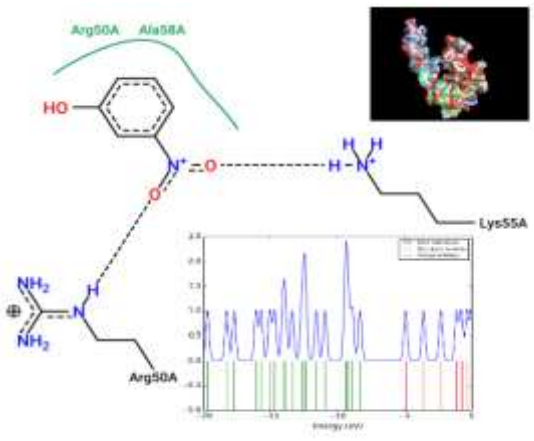

Section: Research Paper

Keywords: MNP, FTIR, FT-Raman, UV-Vis, HOMO-LUMO, MESP and Docking

1. INTRODUCTION

Many fruits and vegetables have naturally coloured pigments due to Phenolic compounds. Polyphenols, which are abundant in wine, tea, grapes, and a wide range of other plants, have been linked to the protection of heart disease and cancer [1]. M-Nitrophenols have significant antioxidant effects due to their Polyphenolic composition and are commonly employed as components in medicinal drugs. M-Nitrophenol is a poisonous and irritating light-yellow crystalline substance. When heated to breakdown, it generates harmful vapours of nitrogen oxides. Despite the presence of a hydroxyl (-OH) group in their structure, phenols acts not like a organic alcohols but they react as mild organic acids. As acids, Phenols and Cresols are far weaker than ordinary carboxylic acids. Strong reducing chemicals such as hydrides, nitrides, alkali metals, and sulphides are incompatible with these materials. Flammable gas (H2) is frequently produced, and the heat created by the process may ignite the gas. The acid-base reaction between phenols and bases also produces heat[2-8]. Gaussian Input file created to undertake geometry optimisation calculations. Moreover, Molecular Orbital reveals valuable insight to determine the Properties of the compound. The selected compound chemical behaviour and molecular characteristics are the key focus of this research.

2. EXPERIMENTAL DETAILS

Without further ado, a sample of M-Nitrophenol with a stated purity of more than 98% was obtained and used as such.A t normal temperature, the sample M-Nitrophenol is in powder form. The sample's FT-IR spectrum was measured between 4000 cm^{-1} to 400 $cm^{-1.}$ A RFS100/S spectrometer used to record the FT-Raman spectrum. An Nd-YAG laser's 1064 nm line was employed as the excitation wavelength in the 3500-50 cm^{-1} range.

3. COMPUTATIONAL DETAILS

The entire computation is performed using the Gaussian09 W[9], the optimised structures' minimum energy conformations were confirmed. At the optimised structure of the M-Nitrophenol, no imaginary frequencies were observed, suggesting that a real minimum on the potential energy was analysed. GIAO technique was used to determine ^{1}H and ^{13}C NMR isotropic shielding using the optimised parameters obtained from the B3LYP/6-311++G(d) approach. The chemical shift and shielding computed by theoretical NMR were incorporated using IEF-PCM (W). The calculated isotropic chemical shifts with respect to tetramethylsilane(TMS) were based on the isotropic shielding

values . To visualize the graphical representations of the orbital modes and Gaussian vibrational modes using in checkpoint files created after successful completion Gaussian Program..

4. RESULTS AND DISCUSSION

4.1. Optimization

The Effective parameters such as length and Angle mentioned in Table 1. Figure 1 depicts the Optimized structure arrangement. Between CH ---O and OH ---H is an optimised structure with a description of intermolecular hydrogen connections. These intramolecular interactions are held together by the structure [11-13]. The global minimum energies determined by MNP are 508.9329 and 511.9573 Hartrees for HF and B3LYP structural optimisations, respectively.

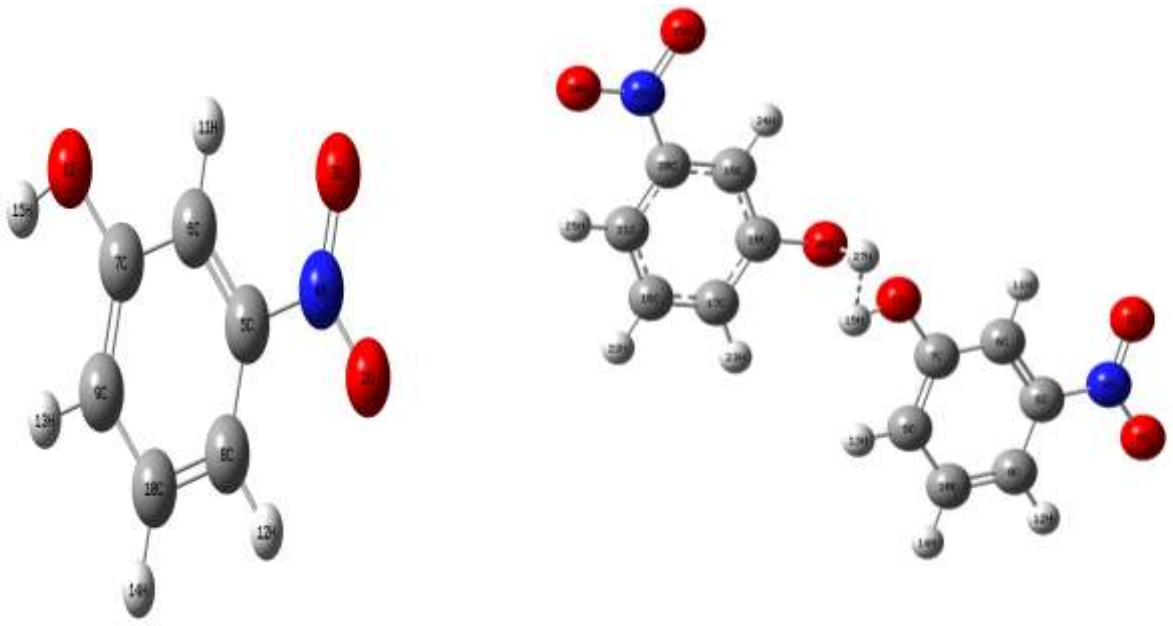

Fig. 1 Monomer and Dimer structure of M-Nitrophenol

Table 1: Structural geomenrty of M-Nitrophenol

Bond length[a]	Value (Å)			Bond Angle[a]	Value (°)		
	HF	B3LYP	*Expt.		HF	B3LYP	*Expt.
O1-C7	1.372	1.3801	1.388	C7-O1-H15	115.6497	115.8415	114.12
O1-H15	0.9464	0.9578	-	O2-N4-O3	123.3566	123.785	-
O2-N4	1.2281	1.2478	1.225	O2-N4-C5	118.2231	118.338	-
O3-N4	1.227	1.301	1.241	O3-N4-C5	118.4203	118.587	-

N4-C5	1.4522	1.468	-	N4-C5-C6	118.3721	118.4217	-
C5-C6	1.3795	1.384	-	N4-C5-C8	118.757	118.857	-
C5-C8	1.3847	1.3876	-	C6-C5-C8	122.8699	122.879	122.25
C6-C7	1.3832	1.4031	-	C5-C6-C7	118.0865	118.1829	118.15
C6-H11	1.0663	1.077	1.089	C5-C6-H11	121.6712	121.6897	-
C7-C9	1.3845	1.3922	-	C7-C6-H11	120.2423	120.4171	-
C8-C10	1.3831	1.3894	1.398	O1-C7-C6	116.4259	116.7478	-
C8-H12	1.0664	1.0771	-	O1-C7-C9	122.9335	122.849	-
C9-C10	1.3885	1.3897	1.399	C6-C7-C9	120.6406	120.7246	-
C9-H13	1.0719	1.0847	1.089	C5-C8-C10	117.8922	117.9112	119.4
C10-H14	1.0697	1.0789	1.089	C10-C8-H12	121.6961	121.7464	-
Intermolecular Bond H15-H27		1.64721	-	**Dihedral angle[a]**			
				H15-O1-C7-C6	180.0107	180.0003	180
				H15-O1-C7-C9	0.0114	0.9955	0
				O2-N4-C5-C6	-179.976	-179.9954	-
				O2-N4-C5-C8	0.0236	-0.0119	-

[a]Refer to Figure 1 for atom numbering.

[*]Ref. [11].

4.2. Vibrational assignments

Based on the measured as well as the theoretically values, vibrational spectral assignments were made. Figures 2 and 3 show the observed spectra, as well as the theoretically spectra and recorded values presented in Table 2. MNP belongs C1 point group symmetry. MNP is made up of 15 atoms and has 39 degrees of freedom in terms of vibration. The 39 normal modes were allocated based on the precise vibrations of individual atoms.

4.2.1.Oxygen–Hydrogen Vibartional Mode Analyses

The O-H stretching vibrations are quite often recorded in the 3550-3200 cm^{-1} range. υO-H is assigned to 3372 the FT-IR bands observed for MNP. The estimated frequencies of the benzene ring's O-H stretching vibrations agree with the experimentally measured values. As predicted, this mode is pure stretching mode, as evidenced by the TED column, and it contributes nearly 100%. The presence of dimeric conventions is caused by hydrogen bonds, which serve as a bridging mechanism.

4.2.2.Carbon–Hydrogen Vibartional Mode Analyses

3100-2800 cm^{-1} is the commonly referred frequency range for υC-H vibrations. The C-H stretching vibrations of the MNP are allocated to the four C-H stretching vibrations 3139,3078,3069, and 3010cm^{-1} with 100% contribution. In-plane C-H bending vibrations occur at frequencies ranging from 1290 to 990 cm^{-1}, whereas out-of-plane bending vibrations occur at frequencies ranging from 940-840 cm^{-1}[14-16]. As a result, the frequencies measured at 1286,1279,1266,1244,1219, and 1209cm^{-1} are ascribed to in-plane bending vibrations, whereas the frequencies seen at 826,802,784 and 732cm^{-1} are assigned to out-of-plane deformation. The interaction between NO_2 and C-H causes a minor divergence in frequency bands.

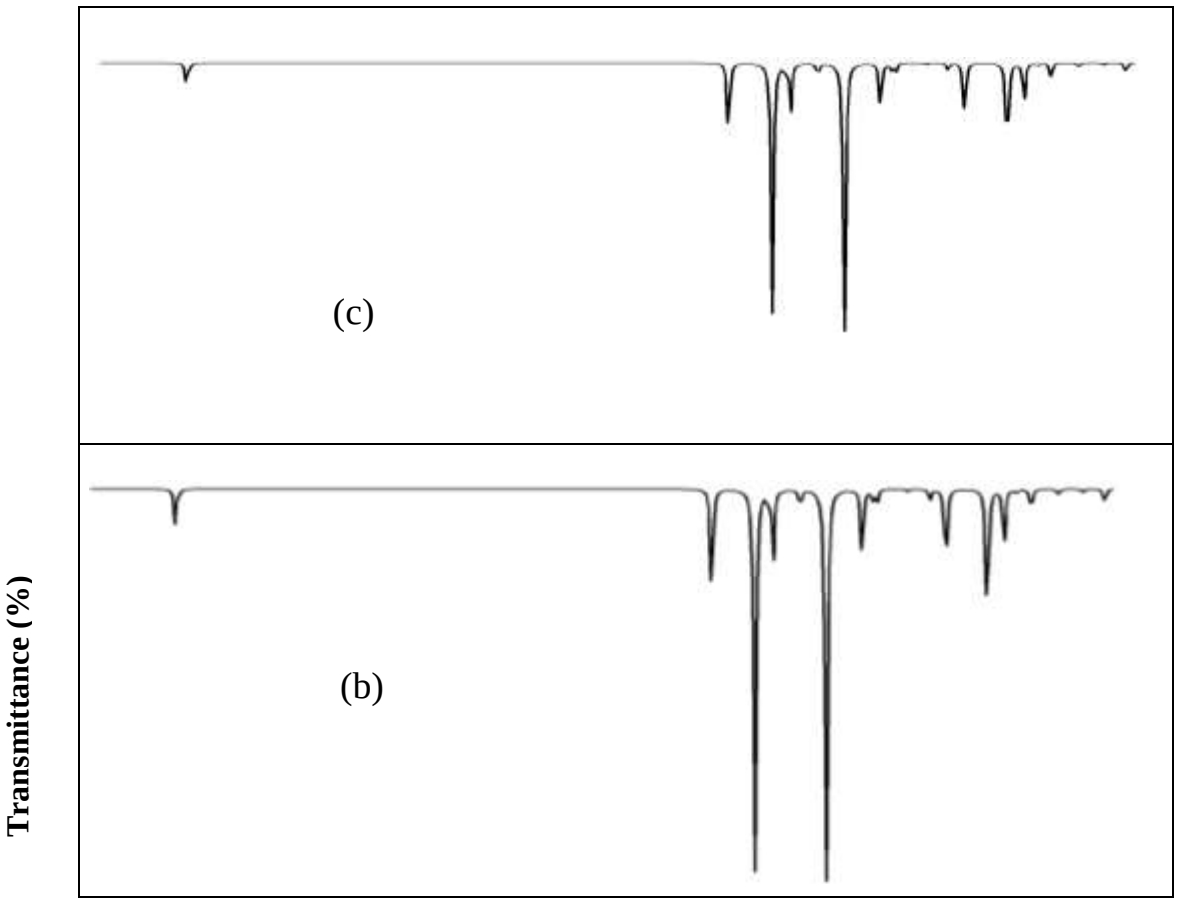

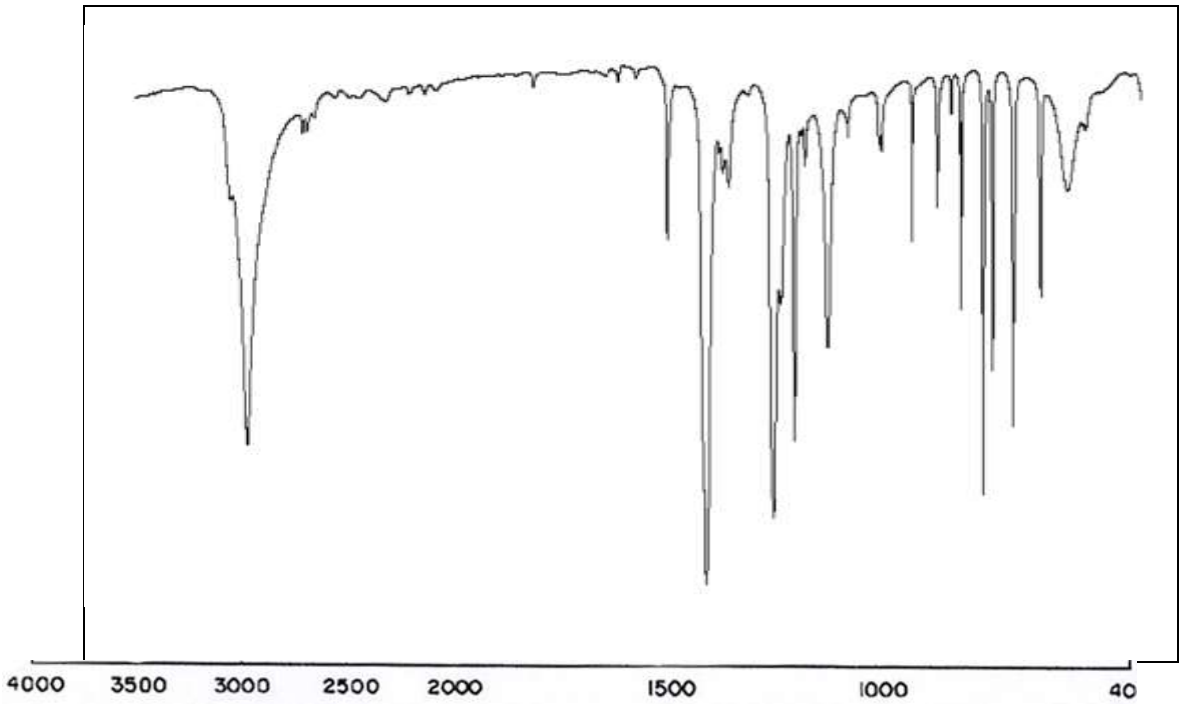

Fig. 2 Comparison of observed and calculated FTIR Spectra of M-Nitrophenol

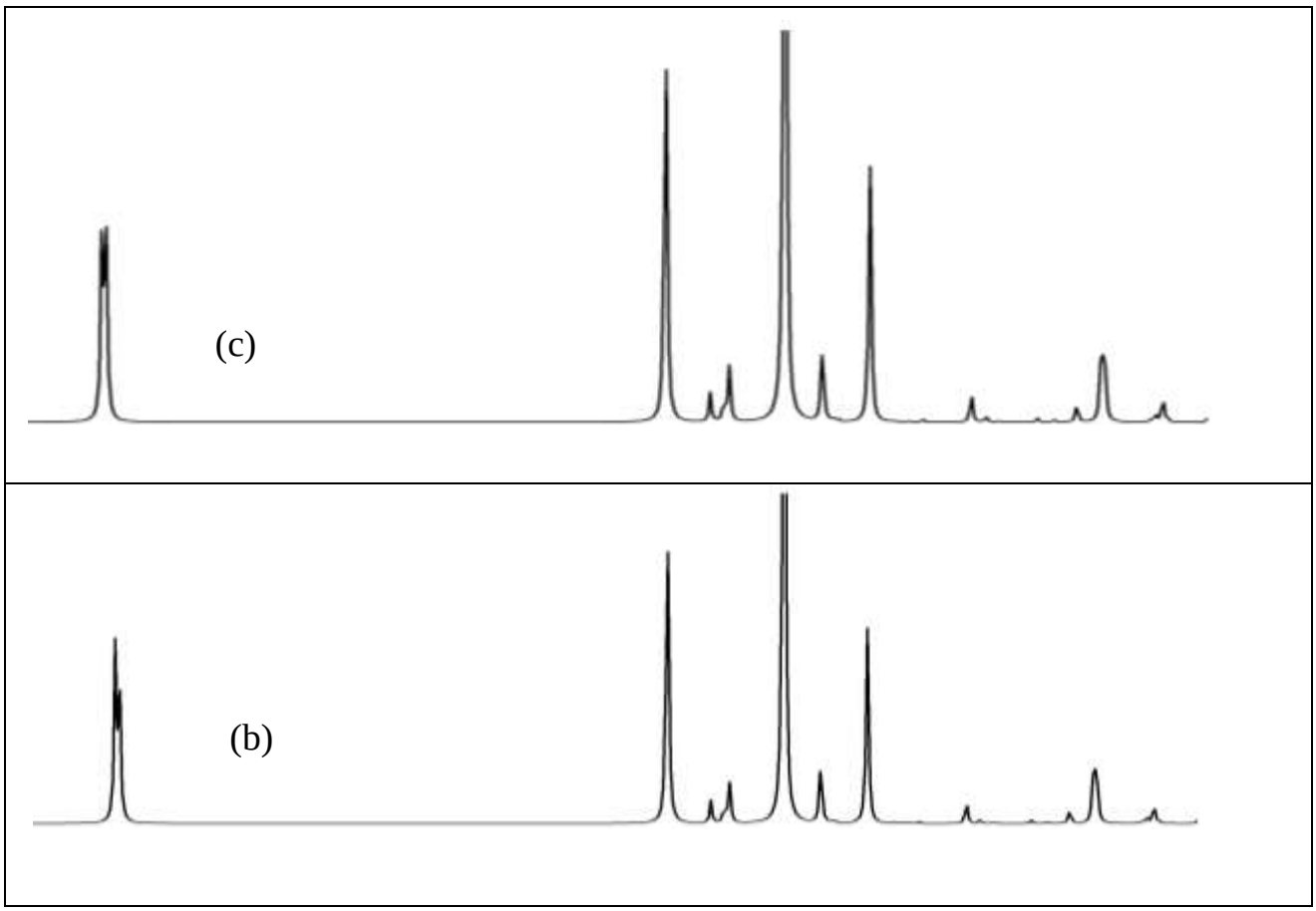

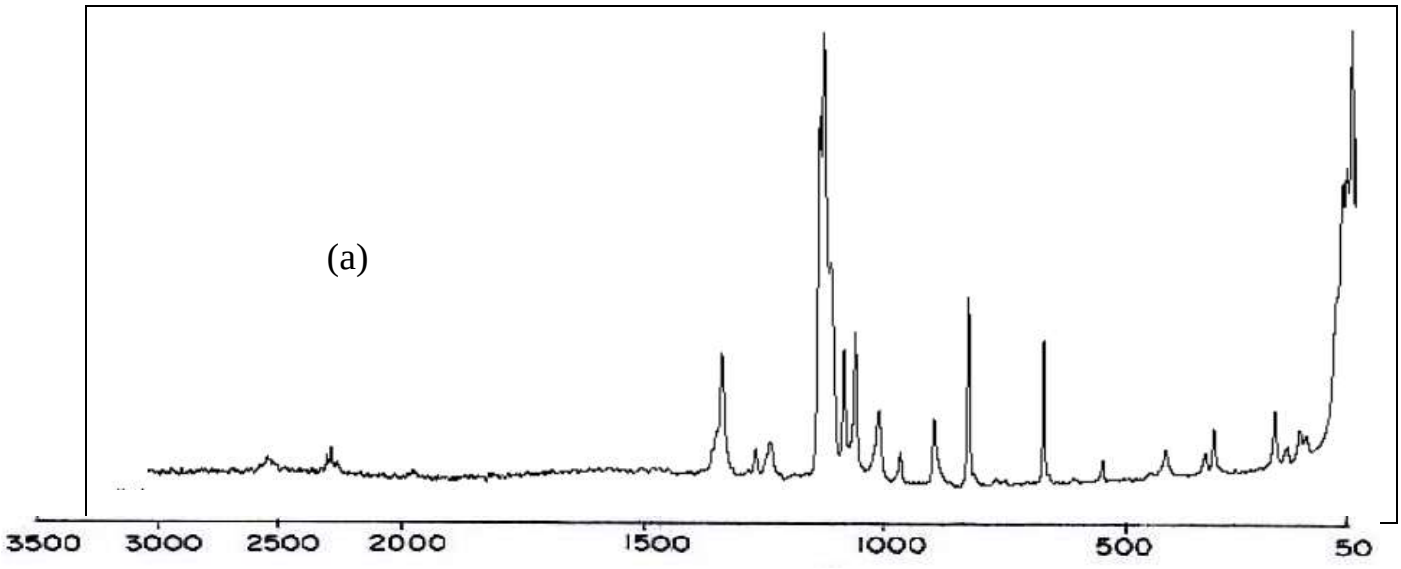

Fig. 3 Comparison of observed and calculated FT-Raman spectra of M-Nitrophenol

Section: Research Paper

Table 2: The Vibrational Modes of M-Nitrophenol

Symmetry Species C_1	Observed frequencies (cm^{-1})		Calculated frequencies (cm^{-1})				IR intensity (KM/Mole)		Raman intensity (A^4/amu)		Assignments with TED (%) among types of internal co-ordinates
			Unscaled		Scaled						
	FTIR	FT-Raman	HF	B3LYP	HF	B3LYP	HF	B3LYP	HF	B3LYP	
A	3372	-	4083	3698	3385	3380	91.7202	56.9614	104.7419	84.1245	νOH(100)
A	3139	-	3414	3239	3153	3150	8.7859	7.9928	47.3150	45.1248	νCH(99)
A	-	3078	3408	3234	3111	3102	2.9166	2.8395	63.3256	60.1789	νCH(99)
A	3069	-	3361	3192	3089	3075	10.4508	10.3043	111.2953	110.1045	νCH(98)
A	3010	-	3330	3164	3025	3017	10.9596	10.9149	74.4724	73.2189	νCH(98)
A	1744	-	1795	1647	1780	1775	27.2509	36.6557	28.3285	27.0178	νCC(63)
A	1697	-	1783	1633	1759	1705	0.0061	11.5825	46.4065	45.0001	νCC (57)

A	1611	-	1662	1528	1625	1615	281.1978	105.5963	1.0382	1.0247	NO_2asym (90)
A	1608	-	1632	1504	1621	1609	10.6242	3.5676	7.4948	7.2367	νCC(74),Rasymd(8),bCH (7)
A	-	1592	1576	1434	1608	1598	363.2685	177.4207	2.4897	2.1478	νCC (67),bCH(12),Rsymd(10)
A	1523	1513	1491	1371	1535	1530	244.9823	17.6802	178.7997	176.0178	νCC(46),bCH(36),CF (6)
A	1453	1459	1453	1340	1487	1468	28.2578	16.8154	2.7088	2.0123	NO_2sym (91)
A	-	1353	1383	1278	1378	1360	35.9564	232.4256	13.4294	12.014	νCC(9),CH(14)
A	1337	-	1374	1267	1348	1340	30.3317	92.2263	5.0400	5.1023	bOH (72)
A	1279	1286	1295	1213	1298	1290	33.2882	3.5131	0.6394	0.6418	bCH (79)
A	-	1266	1241	1172	1278	1270	179.2705	189.0776	4.8064	4.8000	bCH(45),CC(28),CO(9)
A	1244	-	1205	1113	1250	1249	7.8734	17.9197	7.3328	7.3329	bCH(27),Rtrigd(20),CC(9),CO(7)
A	1209	1219	1191	1102	1227	1220	9.5811	9.0101	3.4937	3.4155	bCH(45),CC(28),CO(9)
A	-	1166	1130	1027	1188	1171	0.0038	5.2790	0.1062	0.1041	Rtrigd(5)
A	1151	-	1100	1005	1165	1158	4.1414	0.0137	34.9820	33.0148	Rasymd (22)

A	1069	1073	1062	944	1080	1075	6.6255	11.8998	0.0134	0.0124	Rsymd (22)
A	-	993	1016	926	1025	1011	20.1124	47.7108	0.0769	0.02156	νCN (44)
A	988	-	1009	908	1010	1002	50.4788	11.1663	3.3461	3.3388	νC0 (44)
A	930	-	899	807	998	984	91.6554	78.0650	0.5037	0.4987	NO_2wag (58)
A	872	-	870	785	974	951	59.5943	40.6789	15.012	14.921	ωOH (24)
A	-	826	754	691	878	854	16.6297	5.8648	2.9012	2.7778	ωCH(85),tring(8)
A	802	-	749	690	867	804	9.0327	12.0574	5.0067	4.9140	ωCH(71),gCO(10),tring(8),tRsymd(5)
A	784	-	708	620	798	785	15.5330	5.0185	0.1784	0.1625	ωCH(82),gCN(6),tRasym(5)
A	732	-	688	565	768	754	10.8890	6.4241	1.8918	1.7140	ωCH(85),tring(8)
A	694	-	610	536	725	702	4.2628	4.9006	0.2857	0.2714	NO_2rock (69),Rsymd(9),Rasymd(8)
A	-	673	594	516	704	698	3.0317	0.9192	5.8183	5.7979	tring(59),gCO(10),gCC(9)
A	604	-	556	440	684	612	0.0008	0.0538	0.0484	0.05147	tRasymd(27),bCO(17),Rsymd(12)
A	-	539	483	415	651	599	14.2029	9.6562	2.0631	2.0410	tRsymd(54),Rasymd(13),bCO(11)

A	-	407	450	378	425	412	4.1822	3.0467	0.5685	0.5541	bCN (80)
A	-	394	412	286	402	398	0.0990	156.9059	0.8571	0.8457	bCO(63),bCF(16),Rasymd(7)
A	-	250	261	234	289	265	0.8888	0.0228	0.8547	0.8421	NO_2scis (86)
A	-	210	222	215	271	225	191.5226	0.4671	2.0727	2.0478	ωCN (25)
A	-	184	187	168	201	199	0.2547	0.0284	2.0741	2.0314	ωCO(38)
A	-	171	42	47	185	175	0.1276	0.1762	0.7220	0.7104	NO_2twist (56)

Abbreviations: t - torsion; Rtrigd - Ring trigonal deformation; asym - asymmetric; sym - symmetric; ω - out-of-plane bending; asymd - asymmetric deformation; symd - symmetric deformation; b - in-plane bending;

4.2.3.Carbon-Nitrogen Vibartional Mode Analyses

The Raman band 993 cm^{-1} was assigned the C-N stretching mode. This mode's calculated wavenumber was 1016 cm^{-1}, with a PED contribution of 39% vCN. The DFT calculations demonstrate that the wavenumbers of mixed vibrations, which have 59% C-N stretching mode contributions in Raman spectra [17-18], have 59% C-N stretching mode contributions.

4.2.4.Carbon–Carbon Vibartional Mode Analyses

C-C stretching vibrations are observed at 1744,1697,1608,1592,1523,1513 and 1353 cm^{-1}.

4.2.5. Nitro group vibrational Mode Analyses

Nitro compounds absorb strongly at 1625-1510 cm^{-1} and 1400-1360 cm-^{1} due to the asymmetric and symmetric stretching vibrations of NO_2 [19-24]. The NO_2 asymmetric stretching vibrations were allocated to the IR band detected at 1611 cm^{-1} with high intensity in the current study. The IR and Raman bands detected at 1453 cm^{-1} and 1459 cm^{-1}, respectively, have been ascribed to NO_2 symmetric stretching vibrations. In the area 775-650 cm^{-1}, the NO_2 out-of-plane deformation vibrations show a mild to medium absorption. The band found in the IR spectra for MNP was 654 cm^{-1}. The computed twisting NO_2 vibration is also included.

5. MULLIKEN CHARGES

Carbon, Hydrogen, and Oxygen charges exhibited both signs in the MNP charge distribution. It has both positive and negative charge with typical basic sets. All fundamental sets of donor atoms have negative charges on oxygen atoms. Because of the atomic charge effect,optical,electronic structure, and many other features of molecule systems, mulliken atomic charge plays an ideal role. Polarization causes a charge shift with the origin set[25-27]. Charges of H(13) and H(14) atoms in the MNP are 0.047560e and 0.046187e, respectively. As a result, the charge of the atoms is not affected by the electric field. The Mulliken charge for an individual atom and corresponding values are plotted in Table 3 and Fig 4.

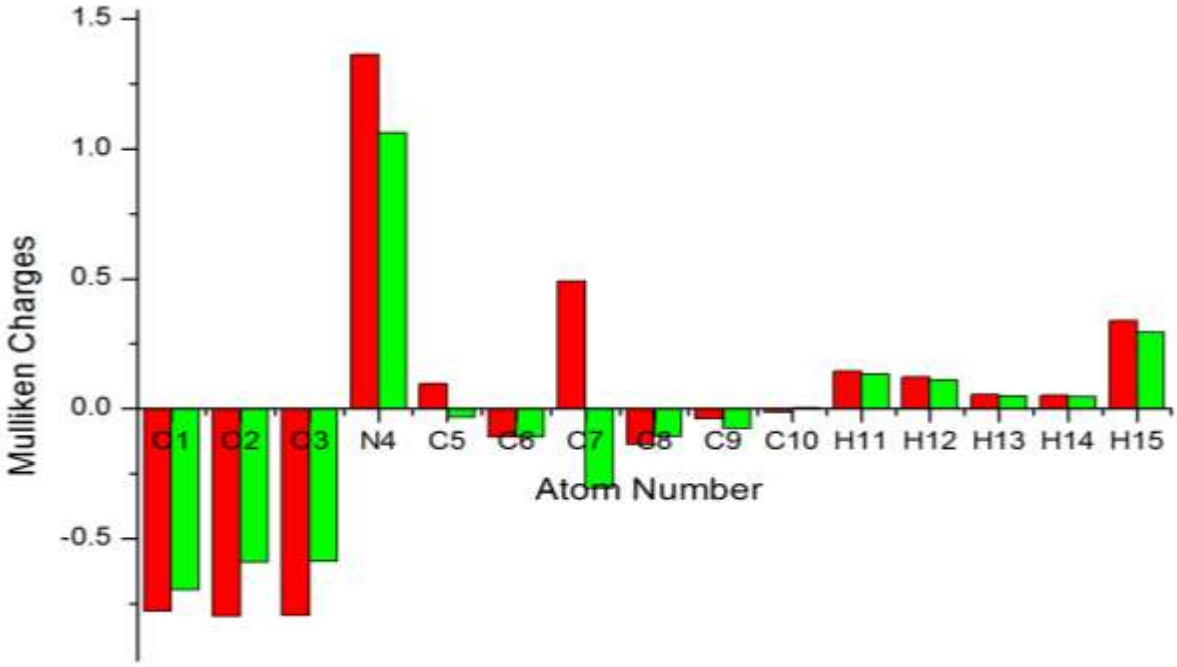

Fig. 4 Plot of Mulliken's charges of M-Nittrophenol

Table 3: The charge distribution of atoms present in the M-Nitrophenol

Atoms No	Atomic charges	
	HF	**B3LYP**
O1	-0.777959	-0.697528
O2	-0.797520	-0.590779
O3	-0.793534	-0.586992
N4	1.362190	1.060829
C5	0.096810	-0.033934
C6	-0.107667	-0.109378
C7	0.490526	-0.305197
C8	-0.136436	-0.105115

C9	-0.037459	-0.075662
C10	-0.013534	0.003722
H11	0.145677	0.133154
H12	0.121622	0.111172
H13	0.055753	0.047560
H14	0.052506	0.046187
H15	0.339024	0.29224

6. Absoption Spectral Analysis

Examination of the absorption reveals that shows two intense peaks of 295.41 and 241.92 nm and transmission spectra shows three intense peaks of 262.12 nm. The spectra showed a high resonance[28-31] that shown in Fig 5 and the transition level,wavelength and the electronic energy values are mentioned in Table 4.

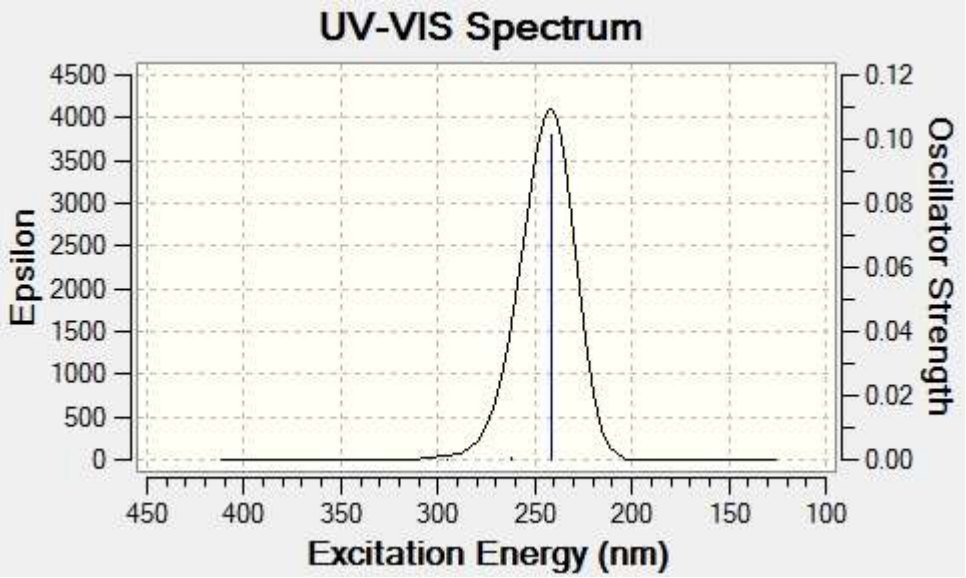

Fig. 5 UV-VIS spectrum of M-Nitrophenol

Table 4: Calculated electronic absorption spectral data of M-Nitrophenol

Excitation	CI expansion coefficient	Wave length (nm)	Oscillator strength (f)	Energy (eV)
HOMO-3 -> LUMO	0.62063	295.41	0.0000	4.1970
HOMO-3 -> LUMO+7	-0.11872			
HOMO-3 -> LUMO+9	-0.21940			
HOMO-4 -> LUMO	0.61833	262.12	0.0000	4.7300
HOMO-4 -> LUMO+7	-0.11721			
HOMO-4 -> LUMO+9	-0.21290			
HOMO-1 -> LUMO+6	-0.16054	241.92	0.1013	5.1250
HOMO -> LUMO	0.65977			

7. First hyperpolarizability

The first hyperpolarizability was computed as 2.1576 10^{-30} esu and 2.1240 10^{-30} esu as presented in Table 5. The computed value of the dipole moment (μ) was 3.0123 Debye. first order hyperpolarizability is 4.540 10^{-30} esu, which is three times that of KDP (β_o= 0.5230 x 10^{-30} esu). The high levels of MNP hyperpolarizabilities, according to the computation, are most likely attributable to charge transfer between the benzene rings inside the molecular skeleton.

8. Transport Properties

Since they are positioned near the compound's outermost limits, these orbitals are frequently referred to as frontier orbitals.The descriptors presented in Table 5. From the table shows that energy gap explains the eventual charge transfer within the molecule. The molecular plots and DOS States are shown in Fig 6 and 7, respectively . The behaviour of

HOMO and LUMO energies, electronegativity, softness, and electrophilic index for MNP is larger than for the benzene, implying that introducing radicals softens the molecule.

Table 5: Molecular and Electronic Properties of M-Nitrophenol.

Parameter	HF	B3LYP
Energy (E)	-508.9329Hartree	−511.9573 Hartree
Dipole moment (μ)	2.9923 debye	3.0123 debye
Polarizability (α)	1.985×10^{-30} esu	1.997×10^{-30} esu
Anisotropy Polarizability (Δα)	2.457×10^{-30} esu	2.568×10^{-30} esu
Hyperpolarizapility (β^{vec})	2.1576×10^{-30} esu	2.1240×10^{-30} esu
μ × β	6.456×10^{-30} esu	6.398×10^{-30} esu
HOMO	9.1906 eV	8.3249 eV
LUMO	5.76270 eV	4.9279 eV
Energy gap (Eg)	3.4279 eV	3.397eV
Electronegativity (χ)	7.47665 eV	6.6264eV
Chemical potential (μ)	-7.47665 eV	-6.6264 eV
Chemical Hardness (η)	1.71395eV	1.6985eV
Softness (S)	0.29172eV	0.29437 eV
Electrophilicity index (ω)	16.3074eV	12.9258eV

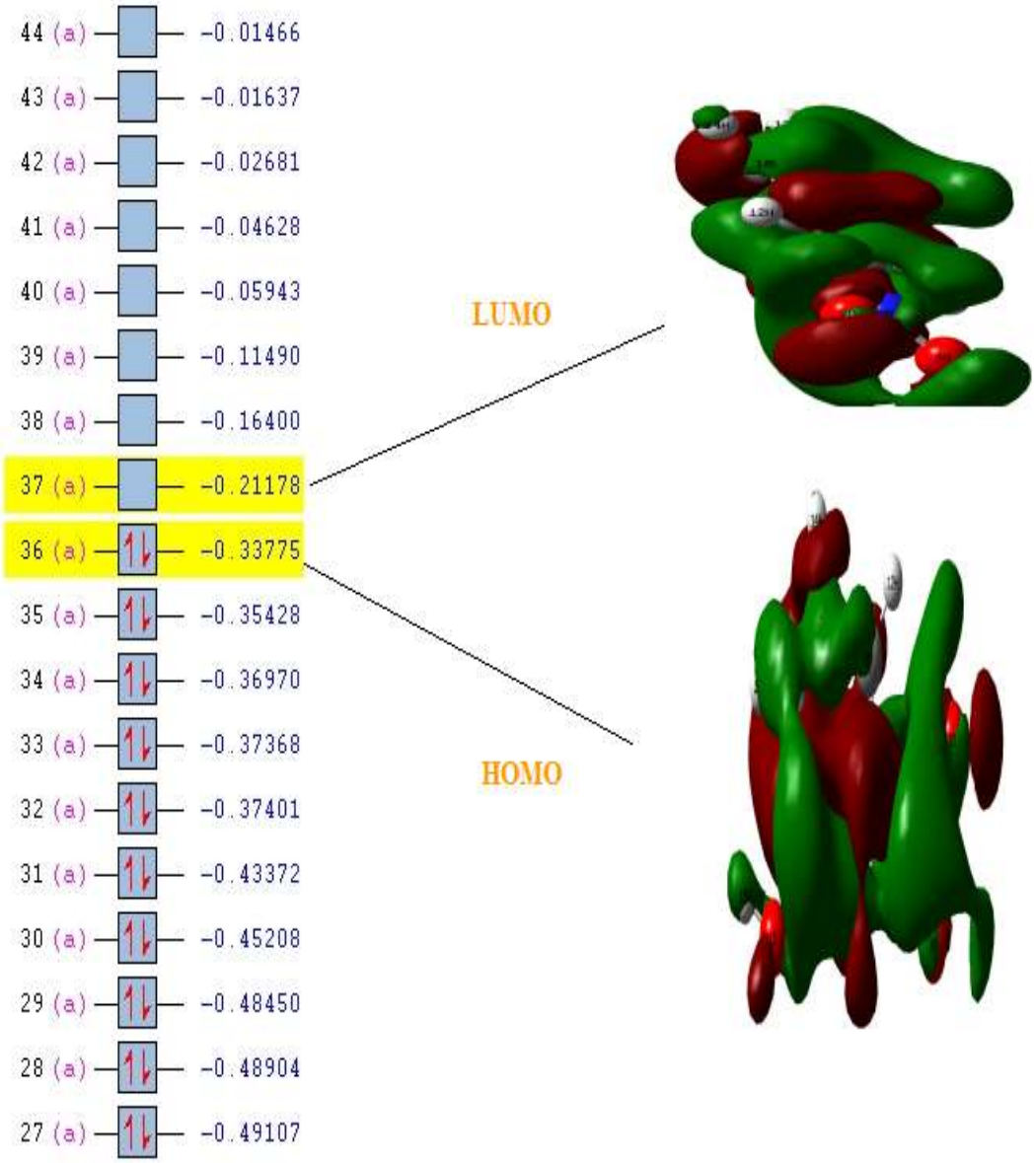

Fig. 6 The frontier molecular orbital for M-Nitrophenol

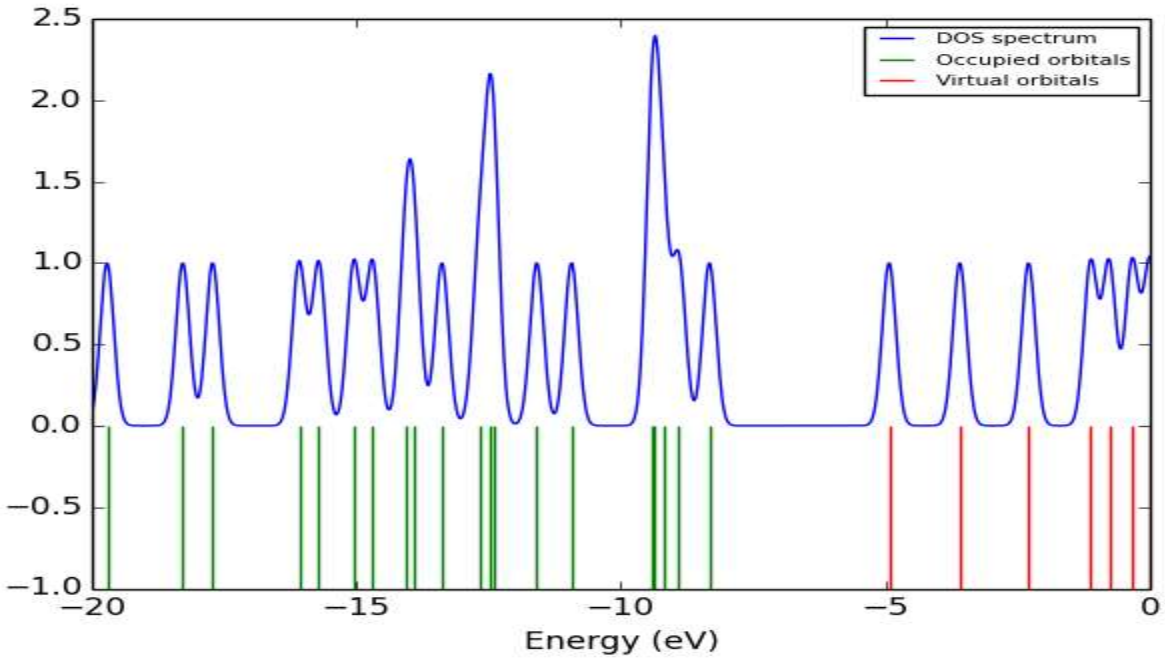

Fig. 7 DOS Spectrum of M-Nitrophenol

9. Molecular electrostatic potential (MEP)

The MEP created a charge distribution gap surrounding the molecule, which is particularly effective in accepting reactive areas in biological identification and hydrogen bonding interactions[36-38]. The zero zones depict the colour green. Figure 8 depicts a graphic depiction of chemically active locations and atoms' comparative reactivity. Various orientations of ESP maps emphasise interactions while also emphasising differences in the type of interactions.

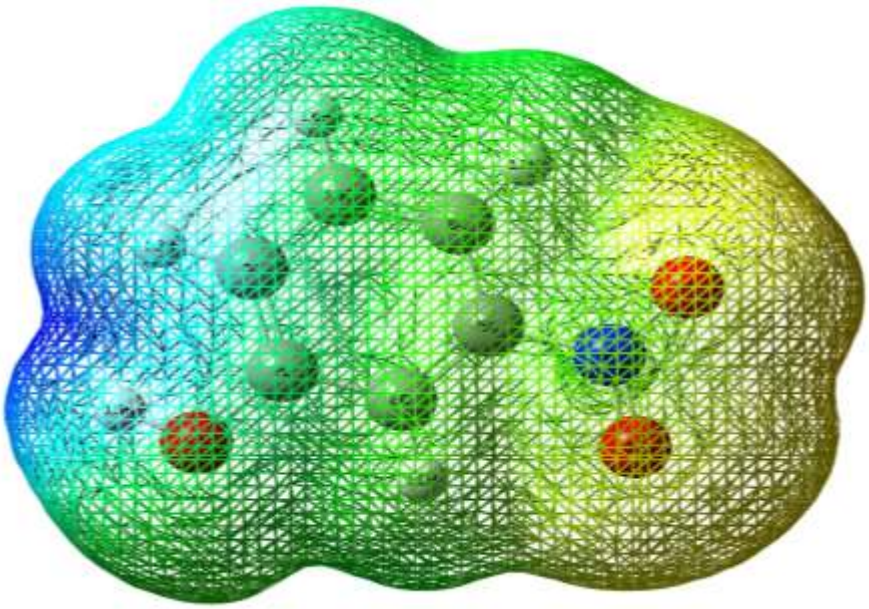

Fig. 8 MEP of M-Nitrophenol

10. ^{13}C AND ^{1}H NMR SPECTRAL ANALYSIS

The shielding of atoms in a molecule is heavily impacted by the neighbouring connected atoms. Same bound atoms offer varying shielding values in various situations. This study looked at the chemical shift values of carbon and hydrogen atoms. The 13C and 1H NMR spectra of MNP are shown in Figure 10. Exhibit 10 shows the results obtained for all carbon atoms excluding range[39-40]. It is necessary to examine carbon atoms with different chemical shift values than the others. A few carbon atoms have shift values in both the upper and lower ranges. This is because the connection established with the electronegative atom stimulates the transfer of the electron cloud surrounding the electronegative atoms from carbon, thereby deshielding the carbon.

^{1}H-NMR spectrum reveals four types of proton signals corresponding to the main functional groups. The ^{1}H-NMR spectrum indicates a broadening signal at = 8.89 ppm that is strongly assigned to Nitro proton (NO_2). The aromatic protons appear in multiples in the area of = 6.82-7.33 ppm, which is predicted. Aromatic carbon atoms may be found in the area between = 111.833 and 155.357 ppm. The ^{13}C-NMR spectra exhibits two singlets at =

155.357 ppm and = 142.833 ppm, which can be assigned to carbon atoms of the (C=N) and (O=H) groups, respectively. Table 6 shows the chemical shift values of MNP.

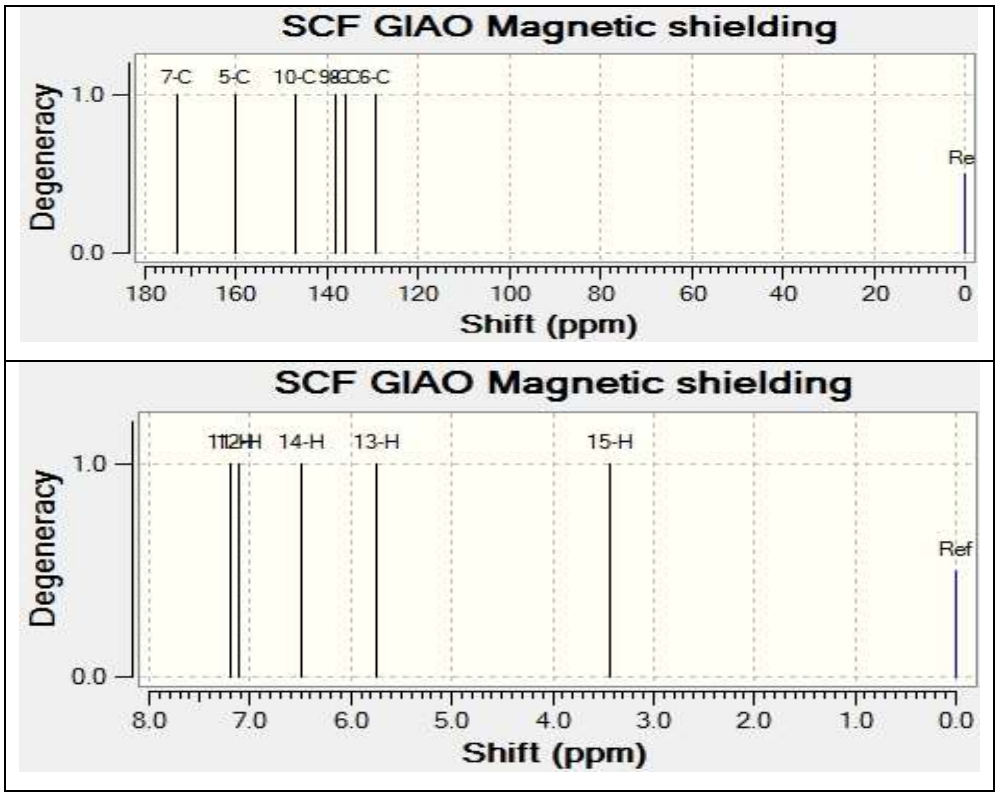

Fig 10 ^{13}C and ^{1}H NMR spectra of M-Nitrophenol

Table 6: The calculated chemical shifts (GIAO method) of M-Nitrophenol

Atoms	Chemical shifts (δ) (ppm)	Isotropic chemical shielding tensor (σ) (ppm)
C5	142.833	

C6	111.833	182.4656
C7	155.357	
C8	118.501	
C9	120.861	
C10	129.632	
H11	7.2036	31.8821
H12	7.1105	
H13	5.7379	
H14	6.4901	
H15	3.4295	

12.Statistical properties

Another essential electrical feature in a molecule is statistical Properties of MNP were computed and presented in Table 7. Because of the high depolarisation of the oxygen lone pair of electrons into the benzene ring and the electron donating Nitro group, MNP has a larger dipole moment. For neutral molecules, dipole moments are the important criteria the interaction strength[41-42]. For example, the stronger the intermolecular interactions, the greater the dipole moment.

Table 7: Thermodynamic properties for M-Nitrophenol

Parameters	**Values**	
	HF	**B3LYP**
Zero-point vibrational energy (kcal mol^{-1})	71.48944	66.23007
Rotational Constants (GH_Z)		
A	2.75076	2.67367
B	0.99879	0.97555
C	0.73274	0.71476
Thermal Energy (kcal mol^{-1})		
Total	76.343	71.354
Translation	0.889	0.889
Rotational	0.889	0.889
Vibrational	74.566	69.576
Entropy (cal mol^{-1} kelvin)		
Total	88.559	89.829
Translation	40.700	40.700
Rotational	29.458	29.535

Vibrational	18.400	19.594
Enthalpy (cal mol^{-1} kelvin)		
Total	28.688	30.944
Translation	2.981	2.981
Rotational	2.981	2.981
Vibrational	22.726	24.982

13. MULLIKEN POPULATION ANALYSIS

Table 8 contains the Mulliken population analysis and dual descriptor, as well as the associated plot (Fig 11). The electron density based on local reactivity descriptors; hardness, softness, and the fukui function are proposed to describe chemical selectivity or reactivity at a given point of a chemical system. Although local hardness has been shown to be a credible intermolecular reactivity descriptor, local softness and the fukui function are more valid intramolecular site selectivity descriptors[43-44].

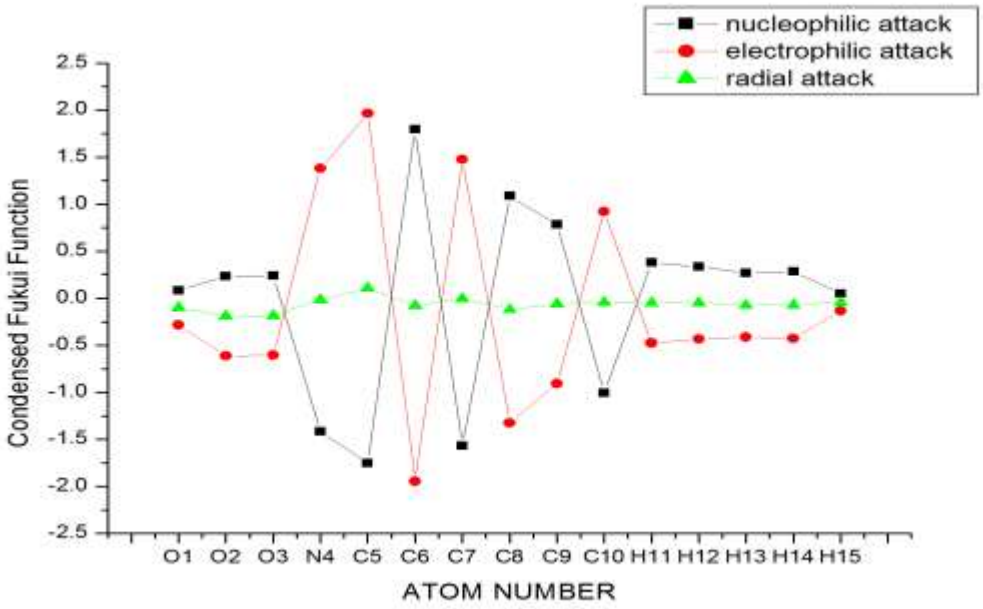

Fig. 11: condensed fukui function plot of M-Nitrophenol

Section: Research Paper

Table 8: Mulliken population analysis calculated at $N_k(N+1)$, $N_k(N-1)$, $N_k(N)$ and condensed fukui function of M-Nitrophenol.

Atom No	$N_k(N+1)$	$N_k(N-1)$	$N_k(N)$	f_k^+	f_k^-	f_k^0
O1	-0.613182	-0.41419	-0.697528	0.084346	-0.283338	-0.099496
O2	-0.355055	0.020000	-0.590779	0.235724	-0.610779	-0.187527
O3	-0.346329	0.016111	-0.586992	0.240663	-0.603103	-0.18122
N4	-0.352913	-0.320943	1.060829	-1.41374	1.381772	-0.015985
C5	-1.783800	-1.998096	-0.033934	-1.7498	1.964162	0.107148
C6	1.684752	1.83454	-0.109378	1.79413	-1.943918	-0.074894
C7	-1.870244	-1.781744	-0.305197	-1.56504	1.476547	-0.004425
C8	0.982258	1.218417	-0.105115	1.087373	-1.323532	-0.118079
C9	0.709719	0.829669	-0.075662	0.785381	-0.905331	-0.05997
C10	-1.006457	-0.917510	0.003722	-1.00273	0.921232	-0.04447
H11	0.513404	0.607598	0.133154	0.38025	-0.474444	-0.04709
H12	0.447776	0.544457	0.111172	0.336604	-0.433285	-0.048340
H13	0.314573	0.461316	0.047560	0.267013	-0.413756	-0.07337
H14	0.330806	0.473450	0.046187	0.284619	-0.427263	-0.071322
H15	0.3446900	0.426928	0.29224	0.05245	-0.134688	-0.041119

13. Docking analysis

Molecular docking simulations were utilised to supplement the molecular level interpretation of the findings in order to enhance experimental efforts. Molecular docking of OPTIFREQ was carried out with Human apolipoprotein C-II in dodecyl phosphocholine (PDB ID: 1SOH) [45] performed using the Auto-Dock Tool (1.5.6). PASS [46] is an internet programme that predicts several sorts of actions. The Protein Data Bank (PDB), (http://www.pdb.org), was used to get human apolipoprotein C-II in dodecyl phosphocholine (PDB ID: 1SOH). and PASS study of OPTIFREQ predicted activities against it. ChemBio 3D ultra 13.0 software was used to create the three-dimensional structure of OPTIFREQ, which was then configured using Gaussian 09W [47] software with the B3LYP/DFT basis package.

LGA and the local search system is used to perform the docking stimulations.The starting location, orientation, and torsion of the ligand molecules were all established appropriately. Upon docking, both rotatable torsion was relieved. During the docking experiment, 10 alternative run sets were designed to achieve an objective. There were 250,000 energy sources analyzed in total. The population limit was set at 150 people. With Gasteiger partial charges, the ligand molecule is identified and added in the same way. The ligand's Torsional Degrees of Freedom (TORSDOF) value is 3, and all rotatable bonds must be stable. Gasteiger provided partial atomic charges to the ligand atoms. A classification of non-polar H-atoms was combined with a representation of rotatable bonds. On a small number of protein targets, docking calculations were performed. Auto Dock tools were used to add the necessary hydrogen atoms. The redemption parameter, as well as the Kollman unified atom type charges, are employed. The Autogrid programme generates affinity grid maps with 112x106x112 grid points and 0.375 A spacing. The Vander Waals and electrostatic terms were estimated using the AutoDock parameter set and distance-dependent dielectric functions. The total additional kollman charge is-36.0, while the total additional gasteiger charge is-36.1314. There are four non-polar hydrogens and six aromatic carbons, each having two rotatable bonds. The ligand and protein were saved in PDBQT format and docked using Autodock. The ligand-receptor interaction had a

magnitude of -10.03 kcal/mol.The active site (ARG50A) N-H bonds, (Lys55A) N-H bonds, of 1SOH and two N-O of OPTIFREQ as well as (ARG50A) N-H bonds of 1SOH and O of OPTIFREQ with bond length of 2.2, 2.2 and 2.5Å, form a hydrogen bond.

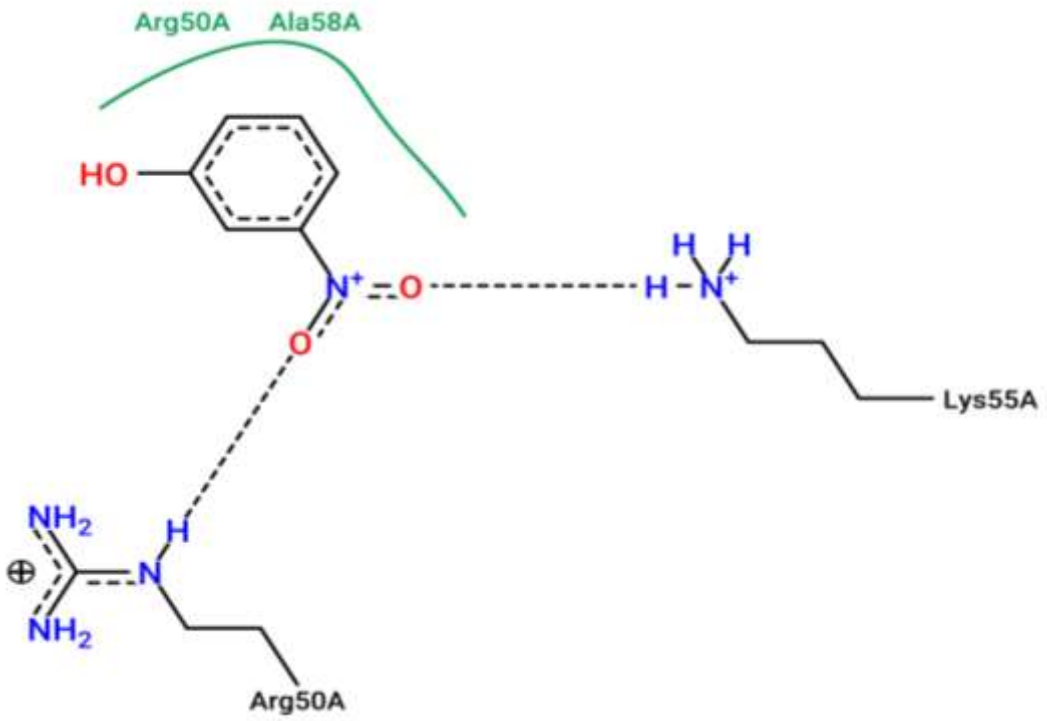

Fig. 12: Poseview diagram of M-Dinitrophenol

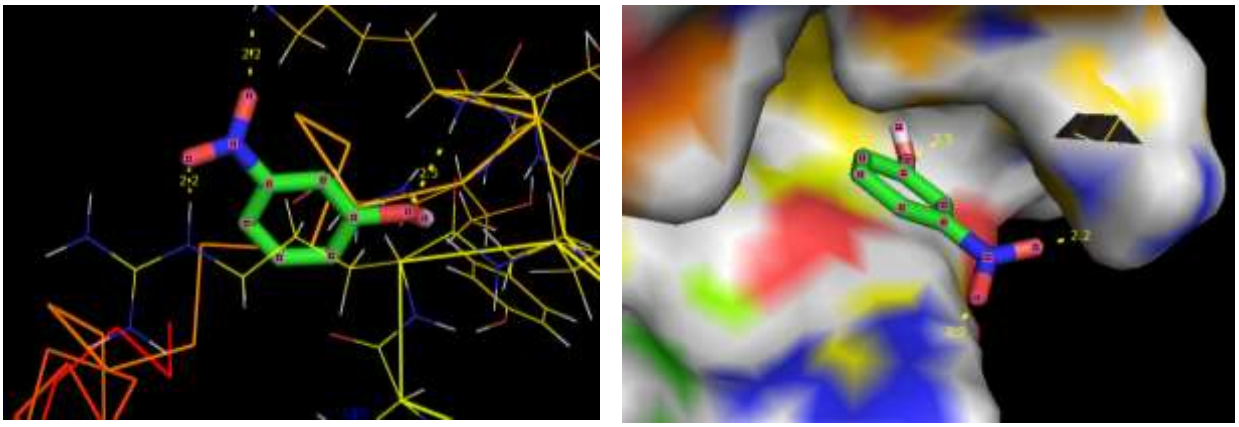

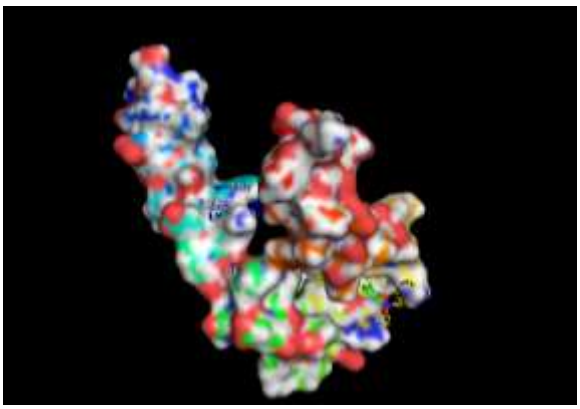

Fig.13: Biological assembly of M-Dinitrophenol

14. Conclusion

Complete material characterization, vibrational mode assignment, HOMO - LUMO analysis, Statistical parameters, reactivity and chemical Shift, potential energy distribution, and Mulliken atomic charges computed using theoretical Calculations. All vibration modes are carefully allocated wavenumbers, which has been determined to be in accordance with our study. The Descriptors transition elucidates CT interaction between the donor and acceptor groups. The MEP plots and corresponding values show that the most reactive regions are found near OH and NO2 groups, whereas, the results clearly reveals the conductivity of MNP is significantly low and the molecule is biological in nature. The Docking analysis four non polar hydrogen are found with six aromatic carbons are found, each with two rotatable bonds. The ligand and protein were saved in PDBQT format and docked using Autodock. The magnitude of the ligand-receptor interaction was -10.03 kcal/mol. The active site (ARG50A) N-H bonds, (Lys55A) N-H bonds, of 1SOH and two N-O of OPTIFREQ as well as (ARG50A) N-H bonds of 1SOH and O of OPTIFREQ with bond length of 2.2, 2.2 and 2.5Å, form a hydrogen bond.

References

1. R. Katritzky, C. W. Rccs, and E. F. V. Scrivcn, *Comprehensive Heterocyclic Chemistry II*, Elsevier, Amsterdam, Netherlands, 1996.
2. Tremp J, Mattrel P, Fingler S, Giger W (1993) Phenols and Nitrophenols as tropospheric pollutants: emissions from automobile exhausts and phase transfer in the atmosphere. Water Air Soil Pollut. 68: 113-123.
3. Luttke J, Levsen K (1997) Phase Partitioning of Phenol and Nitrophenols in clouds. Atmos. Environ. 31: 2649-2655.
4. Zhang DP, Wu WL, Long HY, Liu YC, Yang ZS (2008) Voltammetric Behavior of o-Nitrophenol and Damage to DNA. Int J Mol Sci 9: 316-326.
5. Pedrosa VA, Codognoto L, Avaca LA (2003) Chem. Soc. 14: 530-536.
6. Uberoi V, Bhattacharya SK (1997) Toxicity and degradability of nitrophenols in anaerobic systems. Water. Environ. Res. 69: 146-156.
7. Zaggout FR, Abu Ghalwa N (2008) Removal of o-nitrophenol from water by electrochemical degradation using a lead oxide/titanium modified electrode. J Environ Manage 86: 291-296.
8. Canizares P, Lobato J, Paz R, Rodrigo MA, Sáez C (2005) ElectrochemicalWater Res 39: 2687-2703.
9. M.J. Frisch , G.W. Trucks , H.B. Schlegel , G.E. Scuseria , M.A. Robb , Gaussian 09, C3 revision B.01, Gaussian, Inc., Walling-ford CT, 2010 .
10. A. Frish, A.B. Nielsen, A.J. Holder, GAUSSVIEW user manual, Gaussian Inc., Pittsburg, PA, 2001.
11. Iwasaki F, Kawano Y (1978) ,Acta Crystallogr. B34: 1286-1290.
12. A. Lagunin, A. Stepanchikova, D. Filimonov and V. Poroikov, *Bioinformatics,* 16 (2000) 747.
13. Spectral data base system for Organic compounds: https://sdbs.db.aist.go.jp
14. M. Arivazhagan ,R. Gayathri,Spectrochimica Acta Part A 116 (2013) 170–182.
15. M.K. Subramanian, P.M. Anbarasan, S. Manimegalai, Spectrochim. Acta Part A73 (2009) 642–649.
16. V. Krishnakumar, V.Balachander, Spectrochimica Acta Part A 61 (2005) 2510.

17. R. Anbarasan, A. Dhandapani, S. Manivarman, S. Subashchandrabose, H. Saleem, J. Spectrochim., Acta., 146 (2015) 261.
18. C. James, C. Ravikumar, V.S. Jayakumar, I. Hubert Joe, J. Raman Spectrosc., 40 (2009) 537.
19. S. Pinchas, D. Samuel, M. Weiss-Broday, J. Chem., Soc., (1961) 1688.
20. L. Kahovec, K.W.F. Kohlreusch, Monatsh. J.Chem., 74 (1941) 333.
21. Ruchi Srivastava, L. Sinha, M. Karabacak, O. Prasad, S.K. Pathak, A.M. Asiri, M. Cinar, J. Spectrochim., Acta., 136C (2015) 1205.
22. T. Vijayakumar, H. Joe, C.P.R. Nair, V.S. Jayakumar. J. Chem. Phys., 343 (2008) 83.
23. P. Politzer, J.S. Murray, in: D.L. Beveridge, R. Lavery (EDS,), "Theoretical Biochemistry and Molecular Biophysics": A Comprehensive Survey, Protein, Vol. 2, Adenine Press, Schenectady, NY, 1991 (Chapter 13, Electrostatic Potential Analysis of Dibenzo-p-dioxins and Structurally Similar Systems in Relation to Their Biological Activities).
24. Mahantesha Basanagoud; Susanta K. Nayak; T.N. Guru; Row and Manohar V. Kulkarnia, Acta Crystallographica Section E, 66 (2010) 2780.
25. R.S. Mulliken, J. Chem., Phys., 2 (1934) 782.
26. R.Gayathri,M.Arivazhagan, J.Spectrochim., Acta., 81 A(2011) 242–250
27. T.U. Helgaker, H.J.A. Jensen, P.J. Jorgensen, J.Chem., Phys., 84 (1986) 6280.
28. A. Atac, M. Karabacak, C. Karaca, E. Kose, J.Spectrochim., Acta., 85A (2012) 145.
29. M. Arivazhagan,R.Gayathri, J.Spectrochim., Acta., 116A (2013) 170-182.
30. N.M.O' Boyle, A.L. Tenderholt, K.M. Langner, J. Comp., Chem., 29 (2008) 839.
31. Fiegal. Spot tests in Organic Analysis, Elsevier Publishing co., London, 1960.
32. Kleinman DA (1977) Nonlinear Dielectric Polarization in Optical Media. Phys. Rev. 126: 1962-1979.
33. N. Sundaraganesan, S. Ilakiamani, P. Subramani, B. Dominic Joshua, J. Spectrochim., Acta., 67 A (2007) 628.
34. M. Sekerci, Y. Atalay, F. Yakuphanoglu, D. Avci, A. Basoglu, J.Spectrochim., Acta., 67 A (2007) 503.
35. T.S. Xavier, N. Rashid, I.H. Joe, J.Spectrochim. Acta., 78 A (2011) 319.

36. Tomasi J, Politzer P, Truhlar D (Eds.) (1981) Chemical Application of Atomic and Molecular Electrostatic Potentials, Plenum, New York 257-294.
37. Moro S, Bacilieri M, Ferrari C, Spalluto G (2005) Autocorrelation of molecular electrostatic potential surface properties combined with partial least squares analysis as alternative attractive tool to generate ligand-based 3D-QSARs.Curr Drug Discov Technol 2: 13-21.
38. Murray JS, Sen K (1996) Molecular Electrostatic Potentials, Concepts and Applications, Elsevier, Amsterdam.
39. K.K. Rohatgi-Mukherjee, "Fundamentals of Photochemistry", Wiley, New York, 1978.
40. T. B. Issa, H. Ghalla, S. Marzougui, and L. Benhamada, , *Journal of Molecular Structure*, vol. 1150, pp. 127–134, 2017.
41. C.James, A.Amal Raj, R.Rehunathan, I.H.Joe, V.S. Jayakumar, J.Raman Spectrosc. 37 (2006) 1381-1392.
42. V. Sivagami, M. Karnan and M. Anuradha - Journal of Applied Science and Computations, Volume VI, Issue II, February/2019
43. D. Cecily Mary Glory, K. Sambathkumar, R. Madivanane , G. Velmurugan,R. Gayathri , S. Nithiyanantham, M. Venkatachalapathy, N. Rajkamal J of Molecular Structure 1163 (2018) 480-495.
44. A. Lagunin, A. Stepanchikova, D. Filimonov and V. Poroikov, *Bioinformatics,* 16 (2000) 747.
45. R.Gayathri , J of Molecular Structure 1166 (2018) 63-78.
46. Lagunin, A. Stepanchikova, D. Filimonov and V. Poroikov, *Bioinformatics,* 16 (2000) 747.
47. A. Frisch, R. Dennington II, T. Keith, J. Milliam, A. Nielsen, A. Holder, J. Hiscocks, Gaussview Reference, Version 4.0, Gaussian Inc., Pittsburgh, (2007).